

INTERFACIAL EVALUATION OF ELECTRODEPOSITED CARBON FIBER-EPOXY COMPOSITES BY ELECTRO-MICROMECHANICAL AND NONDESTRUCTIVE TECHNIQUES

Joung-Man Park⁺, Sang-Il Lee and Jin-Won Kim

*Department of Polymer Science & Engineering,
Research Institute of Industrial Technology,
Gyeongsang National University, Chinju, 660-701, Korea
(jmpark@nongae.gsnu.ac.kr)*

SUMMARY: Interfacial and microfailure properties of carbon fiber/epoxy matrix composites were evaluated using both tensile fragmentation and compressive Broutman tests with acoustic emission (AE). Maleic anhydride polymeric coupling agents were used for electrodeposition (ED). ED treatment exhibited higher improvements in interfacial shear strength (IFSS) than untreated case under tensile and compressive tests. The typical microfailure modes including fiber break, matrix cracking, and interlayer failure were observed during tensile test, whereas the diagonal slippage in the fiber ends was observed during compressive test. For both the untreated and treated cases AE distributions were separated well under tensile testing. On the other hand, AE distributions were rather closer under compressive tests because of the difference in failure energies between tensile and compressive loading. Logarithmic electrical resistivity of the untreated or thin diameter carbon fiber composite increased suddenly to the infinity when the fiber fracture occurred by tensile electro-micromechanical test, whereas that of the ED or thick fiber composite increased relatively broadly up to the infinity. Electrical resistance of single-carbon fiber composite increased suddenly due to electrical disconnection by the fiber fracture in tensile electro-micromechanical test, whereas that of SFC increased stepwise due to the occurrence of the partial electrical contact with increasing the buckling or overlapping in compressive test. Electrical resistivity measurement can be very useful technique to evaluate interfacial properties and to monitor curing behavior of single-carbon fiber/epoxy composite under tensile/compressive loading.

KEYWORDS: Interfacial Evaluation, Electrical Resistivity (ER), Electro-micromechanical Technique, Electrodeposition (ED), Residual Stress, Tensile fragmentation test, Compressive Broutman test, Acoustic Emission (AE)

INTRODUCTION

Interfacial shear strength (IFSS) is an important factor to evaluate the mechanical properties in the fiber reinforced composites using both the tensile and compressive fragmentation tests with an aid of AE. The most common micro-mechanical techniques to evaluate IFSS include the single-fiber pullout test [1] and the fragmentation test [2,3] etc. Transversal interfacial properties of the fiber/matrix were obtained by the single-fiber Broutman test to investigate the interface debonding and buckling behavior while subjecting to a transverse compressive stress [4,5]. During both testing, AE test monitored the fracture signals of microfailure sources simultaneously, and correlated with the interfacial shear strength (IFSS). The electrodeposition (ED) to improve IFSS is a process that a polymeric film is deposited on a carbon fiber surface from dispersions of colloid colloidal ion in double-distilled water [6]. During curing process, thermosetting matrix undergoes volume changes resulting from thermal expansion in composite, and matrix shrinkage produce significant residual stress at around fiber. Madhukar [7] studied correlation between matrix volume shrinkage and fiber

tension resulting from residual stress as a function of the thermal history, and proposed optimum cure cycle in various fiber/ thermosetting composites. Recently, several researchers had evaluated curing characteristics by the measurement of electrical resistance. Chung [8] measured electrical resistivity to evaluate curing characteristics and micromechanical properties. The relationship between residual stress and electrical resistivity change during curing was studied in single-carbon fiber/epoxy composite. And then, simultaneous micromechanical properties due to residual stress effect were investigated using electro-micromechanical test. In this work, micro-mechanical technique under tensile and compressive loadings and electrical resistivity measurement were used to evaluate interfacial properties and curing characteristics depending on curing temperature, matrix modulus and the surface treatments in single-carbon fiber/epoxy composites. During the tests, AE signals of microfailure sources are monitored to study their correlation with IFSS.

EXPERIMENTAL

Materials

Carbon fibers with two diameters of 8 μm (Taekwang Industrial Co., Korea) and 18 μm (Mitsubishi Chemical Co., Japan) were used as conductive reinforcing fibers. Testing specimens were prepared with epoxy resin (YD-128, Kukdo Chemical Co., Korea). Epoxy resin is based on diglycidyl ether of bisphenol-A (DGEBA). Polyoxypropylene diamine (Jeffamine D-400 and D-2000, Huntzman Petrochemical Co.) was used as curing agents. Adjusting relative proportion of D-400 versus D-2000 controlled matrix modulus. ED used Polybutadiene-maleic anhydride (PBMA, Polyscience Inc.) as a polymeric coupling agent to improve IFSS.

Methodologies

ED Treatment

Fig. 1 exhibited ED system for carbon fiber surface treatment. Carbon fiber acted as the anode, whereas an aluminum plate was the cathode. After the anode and the cathode were immersed into 0.5 wt.% PBMA aqueous electrolyte solution, 3 voltages were supplied to both electrodes by power supply. Typical coating time was set up for 10 minutes. After ED was treated, carbon fibers were dried at room temperature without further thermal treatment.

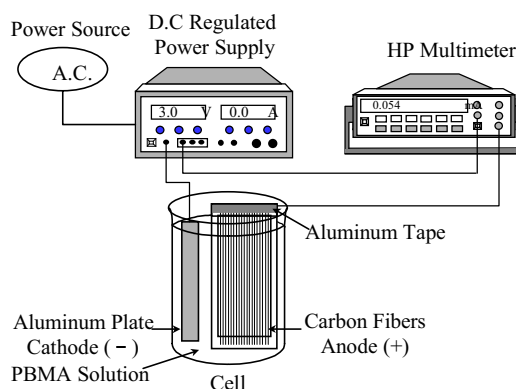


Fig. 1 ED system for carbon fiber surface treatment

Measurements of Mechanical and Electrical Properties of Fibers

About thirty specimens were measured at 20 mm gauge length for each fibers. Universal testing machine (UTM, LR-10K, Lloyd Instrument Ltd.) was used to measure the single-fiber

tensile strength. Electrical resistance was measured at 32 mm in distance between two voltage contacts using digital multimeter.

Preparation of Testing Specimens

Three-type composite specimens were used in this experiment. Fig. 2(a) is a testing specimen to evaluate IFSS using two-fiber tensile fragmentation test. Fig. 2(b) and (c) are single-carbon fiber composites to measure the electrical resistivity under tensile/compressive tests. Testing composites were precured at 80°C for 1 hour and then postcured at 120°C for 1 hour.

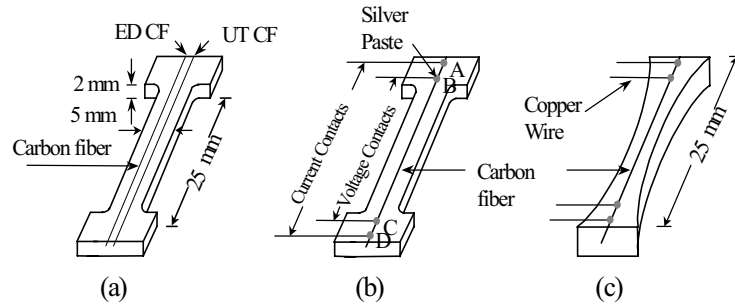


Fig. 2 Three-type testing composites

Measurement of IFSS and Residual Stress

IFSS of carbon fiber/epoxy composite depending on curing temperature, matrix modulus and the surface treatment was measured by tensile/compressive test. Tensile IFSS, τ_t , was determined using Drzal equation [2]. By introducing Weibull distribution for aspect ratio, IFSS was exhibited in the form as follows:

$$\tau_t = \frac{\sigma_{ft}}{2 \cdot \alpha} \cdot \Gamma \left[1 - \frac{1}{\beta} \right] \quad (1)$$

Where α and β are scale and shape parameters of Weibull distribution for aspect ratio (l/d), σ_{ft} is the fiber tensile strength using Weibull weakest link rule, and Γ is gamma function [2]. According to the compressive profile, compressive IFSS, τ_c , based also on the force balance,

$$\tau_c = \frac{\sigma_{fc} \cdot d}{2l_c} \quad (2)$$

where critical length l_c is the original length of the fiber, is σ_{fc} is the fiber stress at the point where the interfacial stress is insufficient to induce further fragmentation. Residual stress was generated by matrix shrinkage due to TEC difference between fiber and matrix during curing process. Residual stress can be obtained by a following equation as [9],

$$\sigma_{residual} = (\alpha_m - \alpha_f) \Delta T \cdot E(\epsilon) \quad (3)$$

Where $E(\epsilon)$ is the elastic modulus resulted from the measures stress/strain response of composite, and α_m and α_f are thermal expansion coefficient of matrix and fiber.

Electrical Resistivity Measurement

In fig. 3, a HP34401A digital multimeter was used to measure electrical resistance during curing or tensile/compressive electro-micromechanical test. Testing speed and load cell were

0.5 mm/minute and 100 kg_f in tensile test and 2 mm/minute and 10KN in compressive test, respectively. Electrical resistance was measured by four-point probe method, and silver paste was used as electrically connecting glue at 4 junctions to maintain electrical contact between the fiber and leading wire (Fig. 2(b)). Total electrical resistance (R_{Tot}) between B and C may include R_c based on the contact resistance by silver paste beside R_f due to the electrical resistance by the fiber as follows:

$$R_{Tot} = R_c + R_f \quad (4)$$

Since the value of R_c is negligibly small due to very high conductivity of silver paste comparing to R_f , it can be considered that the voltage developed between junction B and C becomes nearly fiber resistance,

$$R_{Tot} \cong R_f \quad (5)$$

Electrical resistivity (ρ) was obtained from the measured electrical resistance (R).

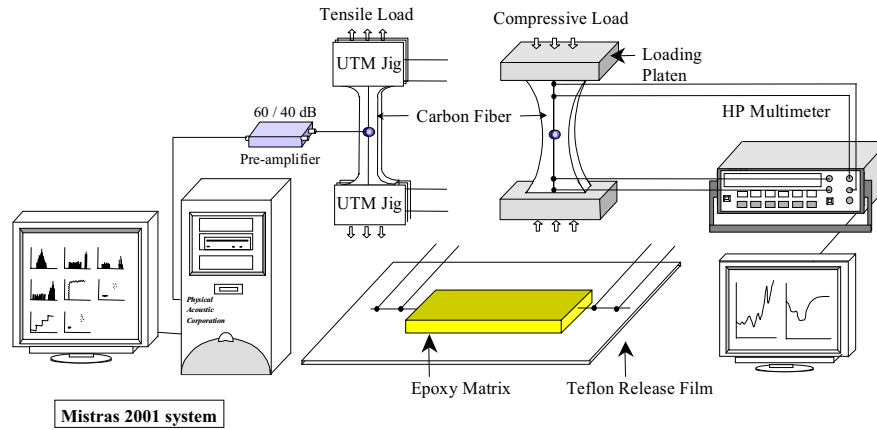


Fig. 3 Acoustic emission and experimental systems for the measurement of electrical resistance

RESULTS and DISCUSSION

Material Properties

Table 1 shows the mechanical and electrical properties of carbon fiber comparing with other fibers. Electrical resistivity of 8 μm carbon fiber was higher than that of 18 μm case due to intrinsic structure of fiber material.

Table 1. Intrinsically electrical and mechanical properties for conductive fibers.

Fiber	Diameter (μm)	Electrical Resistance (Ω)	Electrical ¹⁾ Resistivity ($\times 10^{-3} \Omega \cdot \text{cm}$)	Tensile ²⁾ Strength (MPa)	Elastic Modulus (GPa)
Carbon	8	1.19×10^4 (570) ⁵⁾	18.6 (0.9)	2878	175
Carbon	18	1.57×10^3 (120)	12.5 (1.0)	1753	201
SiC ³⁾	138	0.34×10^3 (10)	156.8 (5.3)	3613	162
Steel ⁴⁾	280	0.57 (0.07)	1.09 (0.1)	1461	193

1, 2) Measured at 32 mm in voltage contacts and 20 mm in gauge length, respectively.

3) Manufactured by Textron Co.

4) No. 1 of guitar string (Segovia Instruments Co., Korea)

5) Parenthesis is standard deviation.

Curing Behavior of SFC

Fig. 4 shows behavior of electrical resistivity depending on curing temperature carbon and steel fiber with or without epoxy matrix. Electrical resistivity decreases as curing temperature in a bare carbon fiber, whereas it increased in a bare steel fiber. It might be due to different fiber structure. In both carbon and steel fiber/epoxy composites, electrical resistance difference (ΔR) is very high compared to two bare fibers. It might be because of residual stress due to matrix shrinkage during curing process.

Fig. 5 exhibits electrical resistivity behavior of single carbon fiber/epoxy composite depending on the curing temperature and matrix modulus. Electrical resistivity difference (ΔR) increased as curing temperature increased. It might be because the curing degree increased at high temperature. In fig. 5(b), ΔR of condition (A) with optimum composition is the largest in same curing temperature, whereas that of condition (B) is the smallest.

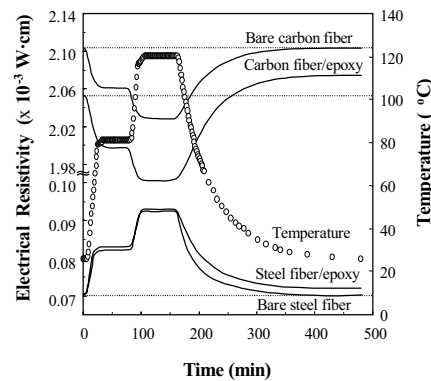


Fig. 4 Behavior of electrical resistivity depending on curing temperature in two bare fibers and SFCs

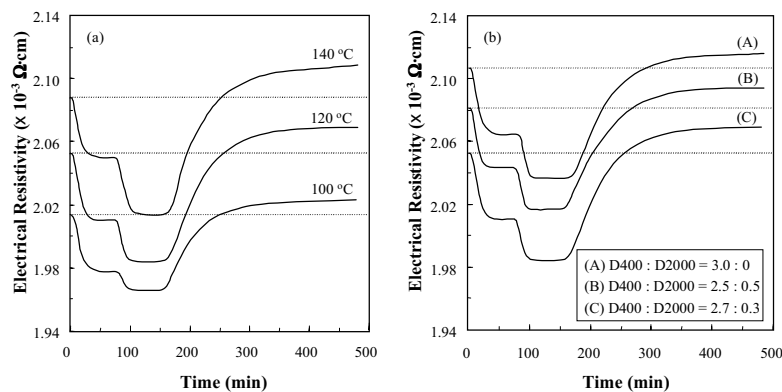


Fig. 5 Electrical resistivity on (a) curing temperature and (b) matrix modulus during curing

Microfailure Modes

In compressive test, the original stress profile along the fiber is entirely unchanged by the fiber fracture, since as the first approximation the compressive stress can be transferred perfectly across the break portion from one fiber fragment to the other. As the compressive stress on the fiber increases further, the fiber will break again at a stress corresponding to the larger compressive strength of the new smaller fragment length in accordance with the strength-length dependence so called as Weibull weakest link rule. An increase in applied strain on the specimen will not result in an increase in the stress on the fiber and hence the fragment length will remain constant. The stress transfer length increases concomitantly at both fiber ends. Unlike in the tensile fragmentation the average fragment length at this point is not related to a critical length as the conventional tensile load transfer model.

The curved-neck specimen under longitudinal compression cause interface debonding to

occur in the transverse direction (i.e., tensile debonding) due to the transverse expansion of the matrix when its Poisson ratio is greater than that of the fiber. The single-fiber compressive test has not been popular as other tensile micro-composite tests because of the problems associated with the difficulties in the specimen preparation and in the visual detection of the onset of interfacial debonding. In order to obtain accurate reproducible results, the fibers should be aligned accurately.

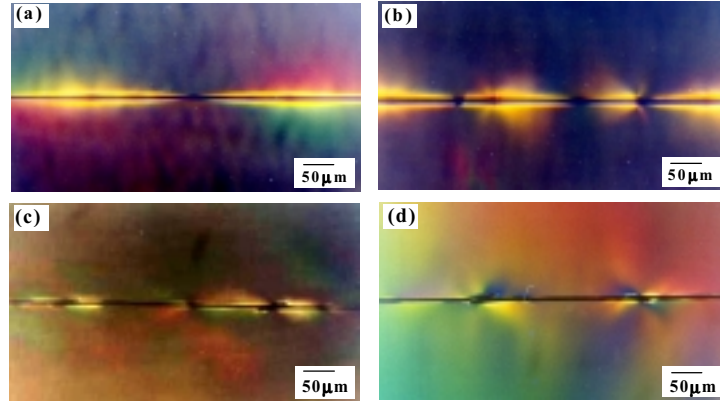


Fig. 6 Polarized-light photograph showing the microfailure modes for (a) untreated (b) ED treated carbon fiber under tensile test; (c) untreated (d) ED treated carbon fiber under compressive test

Fig. 6 shows the photographs of microfailure modes for carbon fiber under tensile and compressive tests. In fig. 6(a) and (b), untreated carbon fiber fracture under tensile test occurred with debonding and low stress whitening was observed around fiber break portion, whereas ED treated carbon fiber occurred with cone-shaped and high stress whitening was observed at fiber break portion. It might be due to the difference in the result of interfacial adhesion. In fig. 6(c) and (d), the diagonal slippage of carbon fiber fracture under compressive test was observed based on transverse tensile stress.

The untreated and the dipping carbon fiber exhibited sharp fractured shape, whereas the ED case exhibited round shaped fracture mode. It is because of the difference in fracture energy between the untreated cases and the ED case. In case of ED case the retarded effect due to the uniform coated layer on the fiber surface.

Interfacial Properties by Tensile/Compressive Electro-micromechanical Test

Fig. 7 shows IFSS between the untreated and ED carbon fiber/epoxy composites by tensile/compressive tests. IFSS of ED case was higher than that of the untreated case in both tests. It might be due to electrical polymer coating layer with chemical or hydrogen bonding.

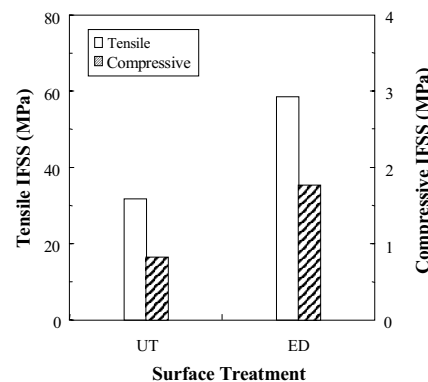


Fig. 7 Comparison of IFSS between the untreated and ED cases using tensile/compressive test

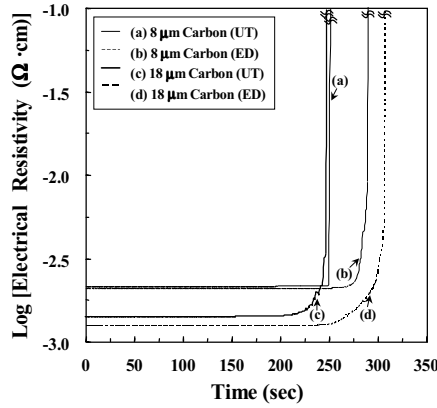


Fig. 8 Logarithmic electrical resistivity of SFC under tensile test

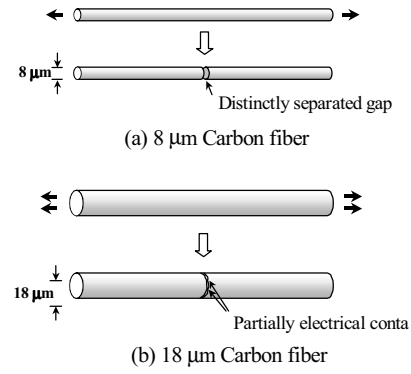


Fig. 9 Schematic model for a fiber breakage with 2 diameters

Fig 8 shows the comparison of logarithmic electrical resistivity depending on the ED treatment in both single 8 and 18 μm carbon fiber composites using tensile electro-micromechanical test. Logarithmic electrical resistivity of the untreated carbon fiber composites increased comparatively suddenly compared to the ED cases. It might be because of the retarded fracture time due to the improved interfacial adhesion. When tensile stress was transferred from matrix to fiber by the external deformation, ED carbon fiber could be endured well against the applied tensile stress and could not be broken easily. When a fiber was broken for the first time, the logarithmic electrical resistivity increased abruptly to the infinity in the case of thin 8 μm carbon fiber composite. On the other hand, the electrical resistivity exhibited smooth increment in the thicker 18 μm carbon fiber composite, and finally the electrical resistivity reached to the infinity. It might be due to the fiber diameter effect by a very abrupt change of the electrical resistivity occurred for thinner 8 μm carbon fiber composite than the thicker 18 μm case.

Fig. 9 exhibited two schematic models for the fiber fracture modes of thin 8 μm and thicker 18 μm carbon fibers in terms of the size effect of fiber diameter. Carbon fiber fracture of 8 μm in diameter shows the complete disconnection, whereas the break of 18 μm carbon fiber shows the maintenance of partial electrical contacts. It was considered that the break of thick 18 μm carbon fiber might be kept on contacting electrically until further strain level comparing to 8 μm case.

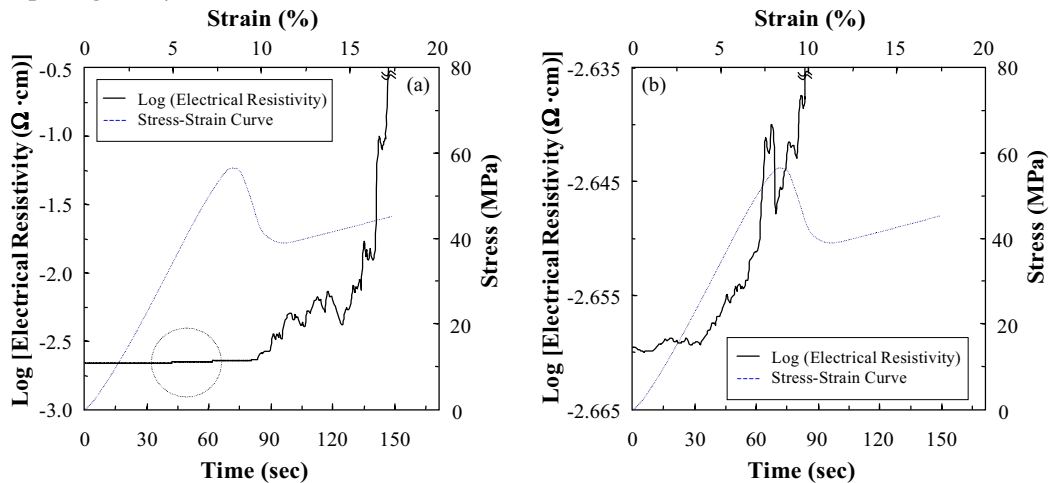


Fig. 10 Logarithmic electrical resistivity of a SFC under compressive load

Fig. 10 shows logarithmic electrical resistivity of single-carbon fiber/epoxy composite by compressive electro-micromechanical test. Fig. 10(a) exhibited total behavior of logarithmic electrical resistivity, and fig. 10(b) was magnified with initial part in fig. 10(a). Significant change of logarithmic electrical resistivity change due to fiber fractures was observed in the initial stage. Change of logarithmic electrical resistivity was large in latter stage. It might be

due to changing contacting distance between fiber fractures. The trend of logarithmic electrical resistivity for single carbon fiber/epoxy composite by compressive test is different significantly from that by tensile test.

Comparison of IFSS and Various Parameters

Fig. 11 shows correlation of IFSS and other parameters in single-carbon fiber/epoxy composites, such as curing temperature and matrix modulus. As curing temperature increase, other parameters except TEC increased. It is considered that residual stress gave effect on the IFSS and electrical resistivity difference. With increasing matrix modulus, TEC decrease whereas other parameters such as IFSS, electrical resistance difference (ΔR), and residual stress increased, and then decreased. It is due to the optimum matrix modulus condition for the maximum performance of composites. It might be due to the optimum matrix modulus condition for the maximum performance of composite.

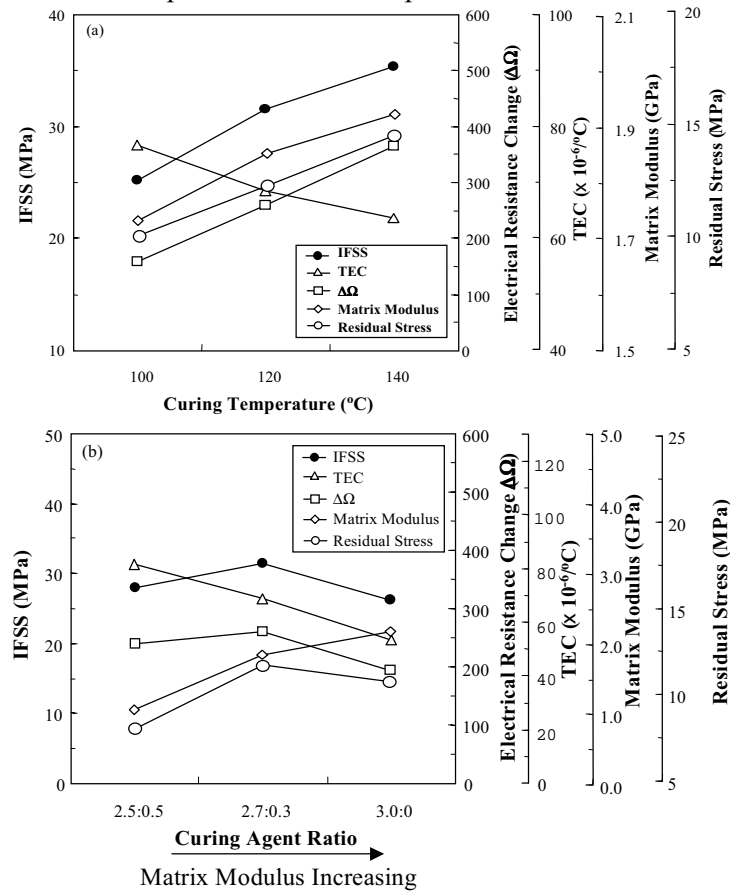


Fig. 11 IFSS and other parameters depending on the (a) curing temperature and (b) matrix modulus

AE Analysis with Microfailure Mechanisms

Fig. 12 shows the stress-strain curves and AE amplitude distributions for carbon fiber/composites using the tensile and the compressive tests. AE amplitudes are separated well in tensile tests for both the untreated and the treated cases in carbon fiber composites, whereas they are rather closely separated in compressive tests. Fracture energy in tensile failure may be much higher than the case in compressive test. Especially, almost 20 dB differences were observed in case of the carbon fiber fracture. It is probably because of the difference in fracture energies between the longitudinal tensile loading in tensile test and the transverse tensile loading in compressive test. For both untreated and treated cases, carbon fiber breaks occurred until just before yielding point under tensile test. Beyond yielding point,

however, much more AE events occurred from the interlayer failure in the ED treated case. Ultimate stress in compressive test exhibited much higher than that of tensile test. All microfailures including fiber break, matrix cracking, and interlayer fracture can be correlated with their inherent material properties.

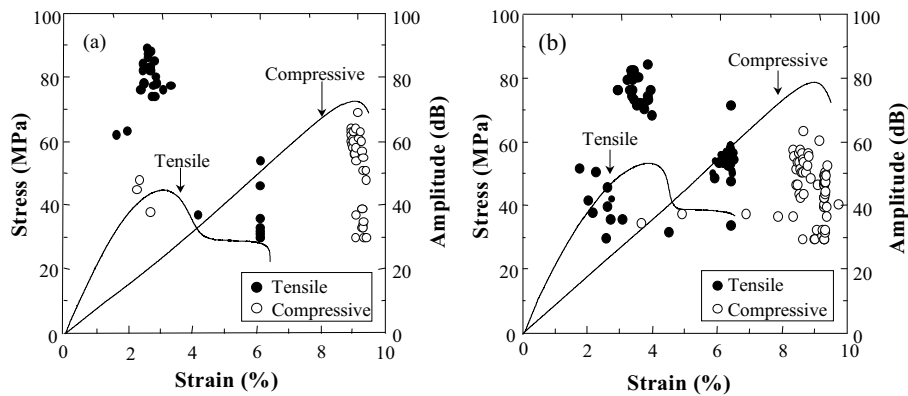


Fig. 12 Stress-strain curves and AE amplitude for carbon fiber/epoxy composites using tensile and compressive tests: (a) the untreated-; (b) ED treated-carbon fiber

Fig. 13 shows AE waveforms in (a) the untreated and (b) ED treated carbon fiber/epoxy composites under tensile and compressive test, respectively. In the case of tensile fragmentation test, there were so many intermediate size waveforms coming from the interlayer failure in the treated conditions. In case of compressive Broutman test, the interlayer failure with intermediate waveform overlapped with carbon fiber fracture signals. The maximum AE voltages coming from the carbon fiber break waveform under tensile tests were much larger than those under compressive tests. Under tensile test ED treated carbon fiber waveform exhibited larger than the untreated case. In compressive test the waveform of ED treated carbon fiber exhibited larger voltage than the untreated case and even than APS treated case. It may be due to the microfailure types and differing failure energies in compressive tests for both the untreated and the treated carbon fibers.

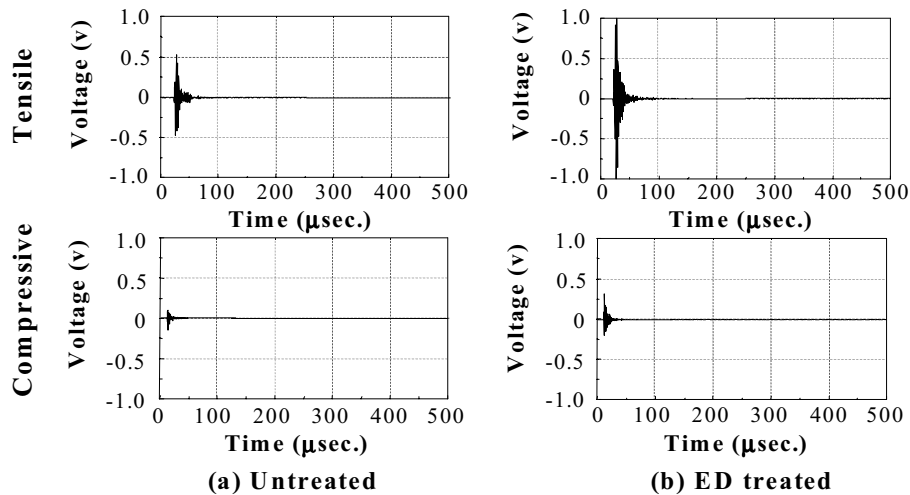


Fig. 13 AE waveform in carbon fiber/epoxy composites: (a) the untreated; (b) ED treated carbon fiber fracture signal under tensile and compressive tests

CONCLUSIONS

Electrical resistance difference (ΔR) of SFC between initial and final stage measured due to residual stress by matrix shrinkage during curing process. As curing temperature and matrix modulus increased, ΔR increased. IFSS of ED composite is relatively higher than the untreated case in the both tensile and compressive tests. It may be due to the interlayer with the compact and more uniform surface coating in ED case. In compressive test for carbon

fiber composites, there were diagonal slippages based on the characteristic of the transverse tensile stress in the interface. Logarithmic electrical resistivity of the untreated or thin fiber case increased suddenly to the infinity, whereas the ED or thick fiber case increased broadly to the infinity in SFC. It might be because of the retarded fracture time by improved interfacial adhesion and fiber diameter effect. In tensile test of single-carbon fiber composite, a sudden increase of electrical resistance exhibited due to electrical disconnection by the fiber fracture, whereas in compressive test the stepwise increase of ΔR was observed due to the occurrence of the partial electrical contact with increasing the buckling or overlapping. As curing temperature increased, TEC decreased, whereas IFSS, electrical resistivity difference, and residual stress increased due to increasing the curing degree by high temperature. In controlling curing agent formulation, IFSS and other parameters such as ΔR and residual stress is largest at optimum curing agent composition, whereas that of brittle matrix is smallest. For both the untreated and the treated cases AE events were separated well under tensile testing, whereas AE distributions were rather closer under compressive tests, due to the difference in fracture energies between two tests. For both tests, carbon fiber breaks occurred around the yielding point. The maximum AE voltage for the waveform of fiber breaks under tensile tests exhibited much larger than those under compressive tests.

ACKNOWLEDGEMENTS

This work was supported financially by a Korea Research Foundation Grant (KRF-99-041-E00499).

REFERENCES

1. Sanadi, A. R. and Piggott, M. R., "Interfacial effects in carbon-epoxies: Part 2 Strength and modulus with short random fibers", *Journal of Material Science*, 1985, Vol. 20, pp. 431-437.
2. Park, J. M., Shin, W. G. and Yoon, D. J., "A study of interfacial aspects of epoxy-based composites reinforced with dual basalt and SiC fibers by means of the fragmentation test and acoustic emission techniques", *Composite Science and Technology*, 1999, Vol. 59, pp. 355-370.
3. Wood, J. R., Wagner, H. D. and Marom, G., "The compressive fragmentation phenomenon: using microcomposites to evaluate thermal stress, single fibre compressive strengths, Weibull parameters and interfacial shear strength", *Proceeding of Royal Society London*, 1996, A 452, pp. 235-252.
4. Ageorges, C., Friedrich, K. and Ye, L., "Experimental to relate carbon-fiber surface treatments to composites", *Composite Science and Technology*, 1999, Vol. 59, pp. 2101-2113.
5. Schüller, T., Beckert, W., Lauke, B., Ageorges, C. and Friedrich, K., "Single fiber transverse debonding: stress analysis of the Broutman test", *Composite Science and Technology*, 2000, Vol. 60, pp. 2077-2082.
6. Park, J. M., Kim, Y. M. and Kim, K. W. "Interfacial properties of ED carbon fiber reinforced epoxy composites using fragmentation techniques and acoustic emission", *Journal of Colloid interface Science*, 2000, Vol. 231, pp. 114-128.
7. Genidy, M. S., Madhukar, M. S. and Russell, J. D., "A feedback system to obtain an optimum cure cycle for thermoset matrix composites", *Proceedings of 29th International SAMPE Technical Conference*, Oct. 28-Nov. 1, 1997, pp. 302-316.
8. Wang, X. and Chung, D. D. L., "Residual stress in carbon fiber embedded in epoxy, studied by simultaneous measurement of applied stress and electrical resistance", *Composites Interfaces*, 1998, Vol. 5, pp. 191-199.
9. Goda, K., Park, J. M. and Netravali, A. N., "A new theory to obtain Weibull fiber strength parameters from a single-fiber composite test", *Journal of Material Science*, 1995, Vol. 30, pp. 2722-2728.